HHS Public Access

Author manuscript

Science. Author manuscript; available in PMC 2016 August 05.

Published in final edited form as:

Science. 2016 February 5; 351(6273): 613–617. doi:10.1126/science.aad5440.

Foxc1 reinforces quiescence in self-renewing hair follicle stem cells

Li Wang[1], **Julie A. Siegenthaler**[2], **Robin D. Dowell**[1,3], and **Rui Yi**[1,*]

[1]Department of Molecular, Cellular, and Developmental Biology, University of Colorado, Boulder, Colorado 80309, USA

[2]Department of Pediatrics, Denver-Anschutz Medical Campus, University of Colorado, Aurora, CO 80045, USA

[3]BioFrontiers Institute, University of Colorado, Boulder, Colorado 80309, USA

Abstract

Stem cell quiescence preserves the cell reservoir by minimizing cell division over extended periods of time. Self-renewal of quiescent stem cells (SCs) requires the reentry into the cell cycle. In this study, we show that murine hair follicle SCs induce the *Foxc1* transcription factor when activated. Deleting *Foxc1* in activated, but not quiescent, SCs causes failure of the cells to reestablish quiescence and allows premature activation. Deleting *Foxc1* in the SC niche of gene-targeted mice leads to loss of the old hair without impairing quiescence. In self-renewing SCs, Foxc1 activates Nfatc1 and bone morphogenetic protein (BMP) signaling, two key mechanisms that govern quiescence. These findings reveal a dynamic, cell-intrinsic mechanism used by hair follicle SCs to reinforce quiescence upon self-renewal and suggest a unique ability of SCs to maintain cell identity.

Maintaining a pool of adult stem cells (SCs) is critical for tissue homeostasis and wound repair throughout an organism's life. Self-renewal, a defining property of SCs, is achieved by either symmetrical or asymmetrical cell division, through which new generations of SCs are produced to replenish the SC pool(1, 2). Some SCs can also be kept in a quiescent state for a prolonged period of time to minimize cell turnover(3). Although it is well documented that cell extrinsic mechanisms such as those mediated by stem cell niche play important roles in governing the transition between quiescence and self-renewal, it is unclear whether there are cell-intrinsic mechanisms that respond to self-renewal and promote dividing SCs to return to quiescence. In this study, we investigated largely synchronized murine hair follicle SC (HFSC) populations during early adulthood to probe this layer of SC regulation.

*Correspondence to: yir@colorado.edu (R.Y.).

The authors declare no conflicts of interest.

SUPPLEMENTARY MATERIALS
Materials and Methods
Figs. S1–S12
Tables S1–S4
References (32–42)

HFSCs reside in an anatomically distinct compartment of the hair follicle, known as the bulge(4–6). During the adult hair cycle, HFSCs periodically go through the phases of activation and quiescence to maintain the SC population and produce new hair follicles(7). The *Foxc1* transcription factor has been previously identified as one of the few genes with dynamic Histone modification patterns in the HFSCs(8) but its expression and function remained unknown. We first monitored *Foxc1* expression during the adult hair cycle using a *Foxc1-LacZ* knock-in mouse(9) and immunofluorescence (IF) staining. We did not observe expression of *Foxc1* in the interfollicular epidermis in any of the stages examined (fig. S1). At the first telogen (~P18), *Foxc1* was absent from the bulge SC compartment but expressed in the infundibulum and sebaceous gland progenitors (Fig. 1A). By anagen III, *Foxc1* was induced in both the basal and suprabasal bulge layers and the inner root sheath (IRS) (Fig. 1B). In mature HFs, *Foxc1* was strongly expressed in the bulge layers and the IRS (Fig. 1C–G). When HFs progressed through the catagen and reached the second telogen (~P47), *Foxc1* was again absent in the bulge (Fig. 1H–J). The induction of *Foxc1* in both the K6+ suprabasal bulge layer (SBL), a putative niche for HFSCs(10), and the CD34+ HFSCs at the basal bulge layer in anagen but not in telogen was confirmed by IF staining (Fig. 1E and J). Furthermore, by examining old mice in which the hair cycle became asynchronized and all different hair cycle stages were observed in a single animal, we validated that the expression of *Foxc1* inherently correlates with the hair cycle (fig. S1).

We then investigated *Foxc1* function by conditionally deleting *Foxc1* (cKO) in the skin. *K14-Cre* deletes *Foxc1* in all skin lineages. *Foxn1-Cre* deletes *Foxc1* in the SBL but not in the HFSCs. *K15-CrePR* deletes *Foxc1* in the HFSCs but not in the SBL upon induction (Fig. 2A, fig. S2). All WT and cKO animals were born at the expected Mendelian ratios (fig. S3A) and developed normal skin neonatally, consistent with the lack of *Foxc1* expression in embryonic skin progenitors (fig. S3B–C).

Compared to the WT HFs, which usually entered anagen at ~P70-P75, the *K14-Cre* cKO HFs had a significantly shortened telogen: the HFs entered anagen prematurely by the middle of the second telogen at ~P64 (as revealed by the darkened skin) and grew hair coat by P70 (Fig. 2B). We then examined HFSC activation in WT and cKO animals during the second adult telogen. At P47, we observed no signs of HF growth or HFSC division. However, loss of the old hair follicle (also known as club hair) was evident (Fig. 2C). By P60, HF growth was initiated in cKO mice as indicated by widespread BrdU incorporation in both the HFSCs and hair germs (HGs: the progenitors to fuel hair growth) (Fig. 2D and F). By P64, whereas cKO animals produced mature HFs, WT animals were still in quiescent telogen (fig. S4A). In the *Foxn1-Cre* cKO in which *Foxc1* was deleted in the SBL but not in the HFSCs, no premature HF growth was observed although the loss of club hair was evident (Fig. 2E left panel). In contrast, in the *K15-CrePR* model in which *Foxc1* was deleted before anagen, premature HF growth was observed without the loss of club hair at P60 (Fig. 2E middle panel and F). In the *K15-CrePR* model in which *Foxc1* was deleted after anagen, neither premature HF growth nor the loss of club hair was observed at P60 (Fig. 2E right panel and F). By dyeing hair at P21 and observing subsequent loss of the dyed hair, we found the club hair was lost late in the second anagen (~P33 to P35) in the *K14-Cre* and *Foxn1-Cre* cKO (fig. S4B–C). Morphological examination showed that the loss of club

hair was correlated with upward movement of the club hair, likely caused by reduced cell adhesion but not by abnormal apoptosis or proliferation of the SBL (fig. S4D–F).

The widespread loss of club hair was further confirmed by flow cytometry analysis, by which HFSCs were detected as *H2BGFP^{hi}/CD34^{hi}/α6^{hi}* and *H2BGFP^{hi}/CD34^{hi}/α6^{lo}* populations in WT skin(5). The *H2BGFP^{hi}/CD34^{hi}/α6^{lo}* population marks a cell population sandwiched between the club hair and the new hair follicle, characteristic of the two-bulge formation in WT skin(5) (fig. S5A). Consistent with the morphological results, we observed a progressive loss of the *H2BGFP^{hi}/CD34^{hi}/α6^{lo}* population in the *K14-Cre* and *Foxn1-Cre* cKO between P30 and P47 (fig. S5B–C). CD34 levels in the KO HFSCs were also reduced (fig. S5D). These data provide evidence for the requirement of *Foxc1* in restricting HFSCs from premature activation and maintaining the club hair. The *Foxn1-Cre* cKO results suggest *Foxc1* is required by the SBL to maintain the club hair. The *K15-CrePR* cKO results reveal an intrinsic requirement of *Foxc1* by HFSCs and suggest that temporal induction of *Foxc1* in the activated HFSCs during anagen is required to reinforce quiescence.

To determine the effect of loss of *Foxc1* on HFSC quiescence, we performed RNA-Seq at P47 when both WT and *K14-Cre* cKO HFSCs were in telogen. Genes associated with quiescence of HFSCs, including Bmp6(11) and Fgf18(12, 13), and HFSC markers(4, 5, 14) including CD34 were among the significantly downregulated genes whereas genes associated with HFSC activation were upregulated in the cKO (Fig. 3A). Signature genes characteristic of quiescent SCs(3) were dysregulated (Fig. 3A). Global analysis revealed that genes involved in cell division were significantly upregulated (fig. S6A). We then confirmed by qPCR the downregulation of *Bmp6, CD34*, and *Fgf18* and the upregulation of cell cycle genes in the HFSCs purified from each model. Consistent with the cell-intrinsic requirement of *Foxc1* in the HFSCs during anagen, changes of gene expression were only observed in the *K14-Cre* and *K15-CrePR* models, in which *Foxc1* was constitutively deleted or specifically deleted in the HFSCs before anagen respectively, but not in the *Foxn1-Cre* and *K15-CrePR* models, in which *Foxc1* was deleted in the SBL but not in the HFSCs or specifically deleted in the HFSC after anagen respectively (Fig. 3B, fig. S7).

Next we performed Gene Set Enrichment Analysis (GSEA) using published HFSC and progenitor datasets(15). Quiescent *Foxc1* KO HFSCs (P47) were more similar to HG progenitors that are poised for activation than to quiescent HFSCs (Fig. 3C, fig. S8). We also observed a strong similarity between *Foxc1* and *Lhx2* cKO HFSCs in their molecular signature (fig. S8). We then performed principal component analysis (PCA) using datasets from the quiescent or activated HFSCs(8, 12, 16), the HGs(12), the transit-amplifying cells (TACs)(8) and our RNA-Seq data. We found that activated HFSCs (P28) and dividing HFSCs destined for differentiation (P20)(16) were intermediate populations between quiescent HFSCs and HG progenitors. The P47 *Foxc1* KO HFSCs were grouped most closely with activated HFSCs and clearly distinct from quiescent HFSCs (Fig. 3D). These data provide a global view for the sensitized cellular state of the *Foxc1* KO HFSCs prior to the premature SC activation.

To determine the mechanism of Foxc1's action, we analyzed differentially expressed genes in *Foxc1* WT and KO HFSCs between P29 and P31, when the HFSCs are activated and

when *Foxc1* is highly expressed. Genes associated with HFSC quiescence, HFSC markers, and adhesion were notably downregulated and cell cycle regulators were strongly upregulated in the cKO, consistent with the observed phenotypes (Fig. 4A, fig. S6B). These data suggest that the transient expression of Foxc1 maintains SC adhesion and promotes the transition back to quiescence when the HFSCs undergo self-renewal.

Next we mapped open chromatin regions and TF occupancy in the WT and KO HFSCs using ATAC-Seq(17). We analyzed published ChIP-Seq data for Sox9(18), Tcf3/4(19) and Lhx2(20) in HFSCs and observed strong overlaps between ChIP-Seq and ATAC-Seq peaks, validating the detection of TF occupancy by ATAC-seq (fig. S9A–C). To determine Foxc1 recognition motifs, we analyzed a Foxc1 ChIP-Seq dataset(21). *De novo* motif discovery retrieved Foxc1 binding sites that were best matched by previously determined Foxa2 and Foxa1 recognition motifs (fig. S9D). Notably, Foxa2 and Foxc1 were validated to bind to the same enhancer sequences(22), consistent with our findings. Both *Foxa1* and *Foxa2* loci are epigenetically silenced in HFSCs (fig. S10), suggesting Foxc1 is responsible for these binding sites. We then intersected our ATAC-seq peaks harboring the Foxc1 recognition motifs with differentially expressed genes ($p<0.01$) in the *Foxc1* KO HFSCs. We identified 104 genes likely to be targeted by Foxc1 (table S1). Among these putative targets, 85 (81.7%) were downregulated in the *Foxc1* KO HFSCs (fig. S9E). Several genes involved in regulating HFSC quiescence were found to contain Foxc1 binding sites in their promoter or enhancer regions, including *Bmp2*(23), *Foxp1*(24), *Nfatc1*(25, 26), *Prlr*(26, 27).

We further dissected pathways that are downstream from Foxc1. Since ATAC-seq provided a comprehensive survey for all TF binding sites in the genome, we analyzed the top TF hits in our ATAC-seq. Overall in the HFSCs, motifs representing AP-1/c-Jun, p63 and CTCF were the most significantly enriched sequences that were detected by ATAC-seq, consistent with high expression levels and the widespread roles of these TFs in the skin (Fig. 4B). However, when we specifically searched the subset of ATAC-seq peaks that cover the differentially expressed (DE) genes identified in the *Foxc1* KO HFSCs against ATAC peaks of non-DE genes, motifs representing Foxc1, Nfatc1, and Smad, reflecting the BMP signaling pathway, were significantly enriched (Fig. 4B). Furthermore, GSEA comparison showed that direct targets of Nfatc1(28) and pSMAD1/5(29) were significantly enriched and largely downregulated in the *Foxc1* KO HFSCs, thus positively linking the *Foxc1* KO HFSCs to the compromised Bmp signaling pathway and loss of Nfatc1 in the HFSCs(29,30) (Fig. 4C). Sixty-six of these genes, including *Bmp2*, *Bmp6*, *Foxp1*, *Inpp4b, Nfatc1* and *Prlr*, were likely co-regulated by Foxc1, Nfatc1 and Smad (Fig. 4D, tables S2–3). Such a combinatorial action of these TFs is illustrated by the *Nfatc1* locus (Fig. 4E). The direct regulation of *Nfatc1*, *Bmp6* and *Hspb8* by Foxc1 was confirmed by ChIP-PCR and qPCR (Fig. 4F–G, fig. S11). Because *Hspb8* was confirmed as a Smad target(29), it is an example co-regulated by Foxc1 and Smad. Overall, 343 out of 421 differentially expressed genes are likely controlled by Foxc1 directly (104) or by Nfatc1 (170) and Smad (328) indirectly, indicating a collaborative gene regulatory network between Foxc1 and Nfatc1 as well as Bmp signaling, two critical regulatory networks governing the quiescence of HFSCs(11, 12, 23, 25, 30, 31).

In conclusion, we have uncovered a dynamic and cell-intrinsic mechanism mediated by *Foxc1* that is induced to promote quiescent SC identity in response to SC activation. Our

findings also suggest that quiescent SCs actively sense the change of their cellular states and utilize transient gene expression to reinforce their identity. Investigation of such adaptive mechanisms should provide new insights into SC maintenance during tissue homeostasis and injury repair.

Supplementary Material

Refer to Web version on PubMed Central for supplementary material.

Acknowledgments

We thank members of the Yi laboratory for discussions, P. Muhlrad and T. Cech for critical reading of the manuscript, Y. Han for FACS, K. Diener and B. Gao for Illumina sequencing, J. Tyler for imaging. We thank E. Fuchs (Rockefeller University) for *K14-Cre* and *K14-H2BGFP* mice, H. Chang (Stanford University) for help on ATAC-seq, N. Manley (University of Georgia) for *Foxn1-Cre* mice, D. Roop and G. Bilousova (University of Colorado, Denver) for Krt6 antibody. This project was partly supported by NIH grant AR066703 and a start-up fund from the University of Colorado Boulder to R.Y. L.W. was supported by an NIH training grant T32GM008759. R.Y. and R.D.D. were co-advisors for L.W. All sequencing data are deposited to GEO with the accession number GSE67404 and GSE68288.]

References and Notes

1. Orford KW, Scadden DT. Nat Rev Genet. 2008; 9:115–128. [PubMed: 18202695]
2. He S, Nakada D, Morrison SJ. Annu Rev Cell Dev Biol. 2009; 25:377–406. [PubMed: 19575646]
3. Cheung TH, Rando TA. Nat Rev Mol Cell Biol. 2013; 14:329–340. [PubMed: 23698583]
4. Tumbar T, et al. Science. 2004; 303:359–63. [PubMed: 14671312]
5. Blanpain C, Lowry WE, Geoghegan A, Polak L, Fuchs E. Cell. 2004; 118:635–48. [PubMed: 15339667]
6. Cotsarelis G, Sun TT, Lavker RM. Cell. 1990; 61:1329–37. [PubMed: 2364430]
7. Blanpain C, Fuchs E. Nat Rev Mol Cell Biol. 2009; 10:207–17. [PubMed: 19209183]
8. Lien WH, et al. Cell Stem Cell. 2011; 9:219–232. [PubMed: 21885018]
9. Kume T, et al. Cell. 1998; 93:985–996. [PubMed: 9635428]
10. Hsu YC, Pasolli HA, Fuchs E. Cell. 2011; 144:92–105. [PubMed: 21215372]
11. Oshimori N, Fuchs E. Cell Stem Cell. 2012; 10:63–75. [PubMed: 22226356]
12. Greco V, et al. Cell Stem Cell. 2009; 4:155–69. [PubMed: 19200804]
13. Kimura-Ueki M, et al. J Invest Dermatol. 2012; 132:1338–1345. [PubMed: 22297635]
14. Morris RJ, et al. Nat Biotechnol. 2004; 22:411–7. [PubMed: 15024388]
15. Subramanian A, et al. Proc Natl Acad Sci. 2005; 102:15545–15550. [PubMed: 16199517]
16. Zhang YV, Cheong J, Ciapurin N, McDermitt DJ, Tumbar T. Cell Stem Cell. 2009; 5:267–278. [PubMed: 19664980]
17. Buenrostro JD, Giresi PG, Zaba LC, Chang HY, Greenleaf WJ. Nat Methods. 2013; 10:1213–1218. [PubMed: 24097267]
18. Kadaja M, et al. Genes Dev. 2014; 28:328–341. [PubMed: 24532713]
19. Lien WH, et al. Nat Cell Biol. 2014; 16:179–190. [PubMed: 24463605]
20. Folgueras AR, et al. Cell Stem Cell. 2013; 13:314–27. [PubMed: 24012369]
21. Amin S, et al. Dev Cell. 2015; 32:265–277. [PubMed: 25640223]
22. Yamagishi H, et al. Genes Dev. 2003; 17:269–281. [PubMed: 12533514]
23. Plikus MV, et al. Nature. 2008; 451:340–344. [PubMed: 18202659]
24. Leishman E, et al. Dev Camb Engl. 2013; 140:3809–3818.
25. Horsley V, Aliprantis AO, Polak L, Glimcher LH, Fuchs E. Cell. 2008; 132:299–310. [PubMed: 18243104]

26. Goldstein J, et al. Genes Dev. 2014; 28:983–994. [PubMed: 24732379]
27. Craven AJ, et al. Endocrinology. 2001; 142:2533–2539. [PubMed: 11356702]
28. Keyes BE, et al. Proc Natl Acad Sci U S A. 2013; 110:E4950–4959. [PubMed: 24282298]
29. Genander M, et al. Cell Stem Cell. 2014; 15:619–633. [PubMed: 25312496]
30. Kobielak K, Stokes N, de la Cruz J, Polak L, Fuchs E. Proc Natl Acad Sci U A. 2007; 104:10063–8.
31. Botchkarev VA, et al. Nat Cell Biol. 1999; 1:158–164. [PubMed: 10559902]

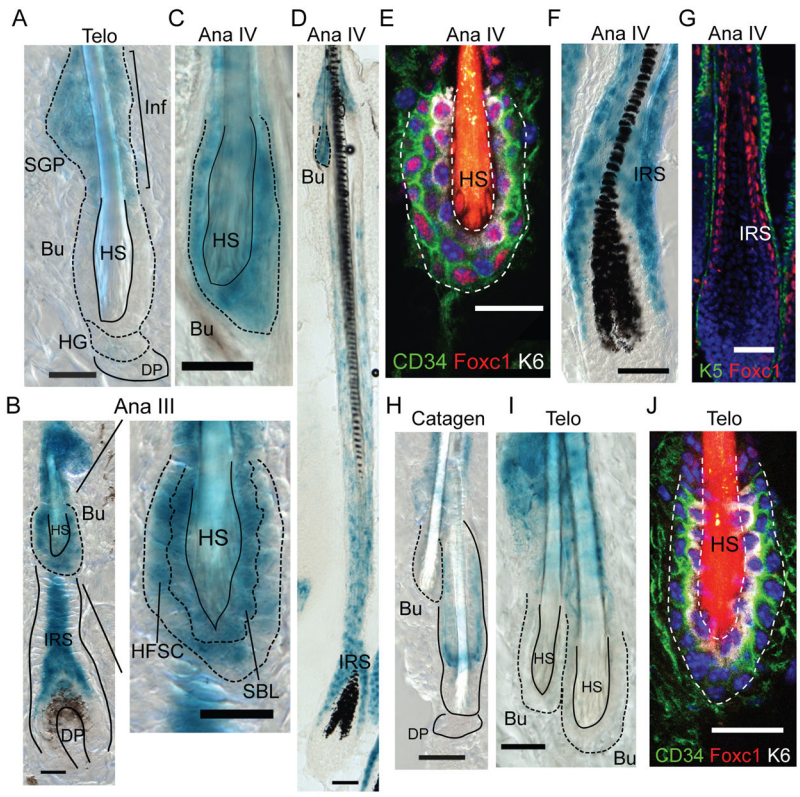

Fig. 1. Dynamic expression of *Foxc1* in the bulge

(A) In telogen, *Foxc1* expresses in the Inf and SGP but not in the bulge. **(B)** *Foxc1* is induced in the HFSC, the SBL, and the IRS at anagen III. **(C–G)** In mature HF of anagen IV, *Foxc1* is highly expressed in the bulge and the IRS. Note in **(E)** *Foxc1* is specifically detected in both K6+ SBL and CD34+ HFSCs and in **(G)** *Foxc1* is detected in the IRS. **(H–I)** There is no *Foxc1* expression in the bulge during catagen and telogen. **(J)** No *Foxc1* expression in telogen bulge is confirmed by IF staining. Inf: infundibulum; SGP: sebaceous gland progenitors; Telo: telogen; Ana: anagen; Bu, bulge; HG, hair germ; DP, dermal papillae; HS, hair shaft; Scale bar 20μm in **A–C** and **E–J**; 50μm in **D**.

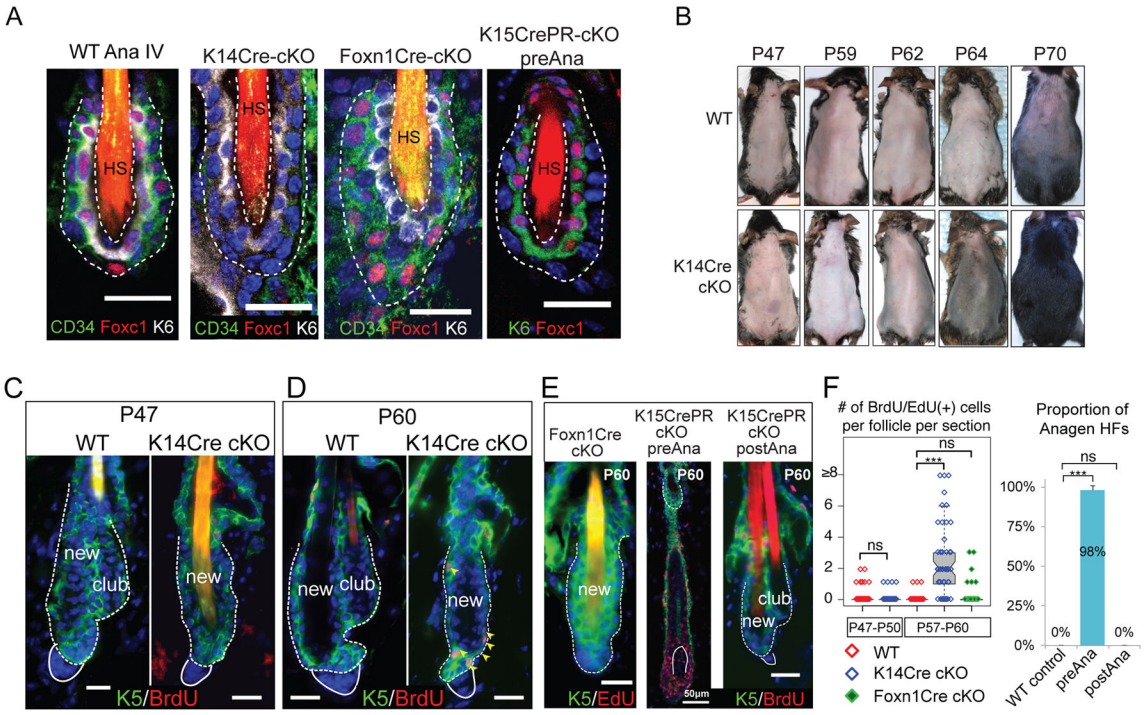

Fig. 2. *Foxc1* is differentially required by the HFSCs and the suprabasal bulge layer

(A) Differential deletion of *Foxc1* by different Cre lines at anagen (P26~P30). **(B)** Premature HF growth of *Foxc1* cKO animals, compared to WT animals, during the second telogen. **(C–D)** Premature HFSC activation in *Foxc1* cKO is shown by BrdU incorporation and HF growth and the loss of club hair in the *K14-Cre* cKO. **(E)** Different defects in club hair loss and compromised quiescence are observed in *Foxn1-Cre* and *K15-CrePR* models. **(F)** Quantification of BrdU or EdU+ cells in the HFSCs and HG cells before (P47–P50, n=3 for each genotype) and after (P57–P60, n=3 for *K14-Cre* n=4 for *Foxn1-Cre*) the premature HFSC activation and quantification of premature HF growth in the *K15-CrePR* model with pre-anagen deletion, compared to the WT and the *K15-CrePR* model with post-anagen deletion. *** p<0.001, ns: not significant. Scale bar 20μm in **A, C–E** unless otherwise labeled. Dotted lines outline the bulge and solid lines outline the DP.

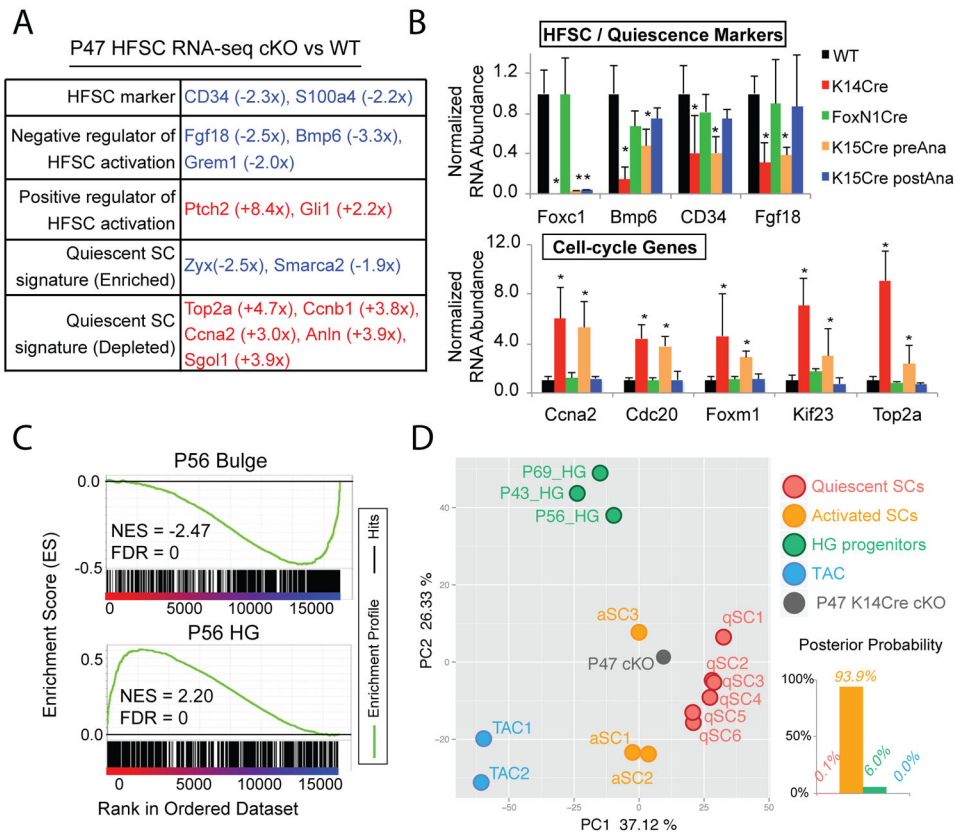

Fig. 3. *Foxc1* KO HFSCs fail to return to quiescence

(A) Functional classification of selected differentially expressed gene in P47 KO HFSCs. Red and blue mark up- and downregulated genes in the KO HFSCs, respectively. **(B)** qPCR validation of down- and upregulated genes in the HFSCs isolated from different cKO models at the second telogen (P47~P60, n≥3 for each genotype, *p<0.05). **(C)** GSEA comparison of P47 KO transcriptome to telogen bulge and HG signature genes. **(D)** PCA of P47 *Foxc1* KO transcriptome and profiling data from WT HFSCs, HGs and TACs. Linear discriminant analysis groups *Foxc1* KO transcriptome to activated HFSCs.

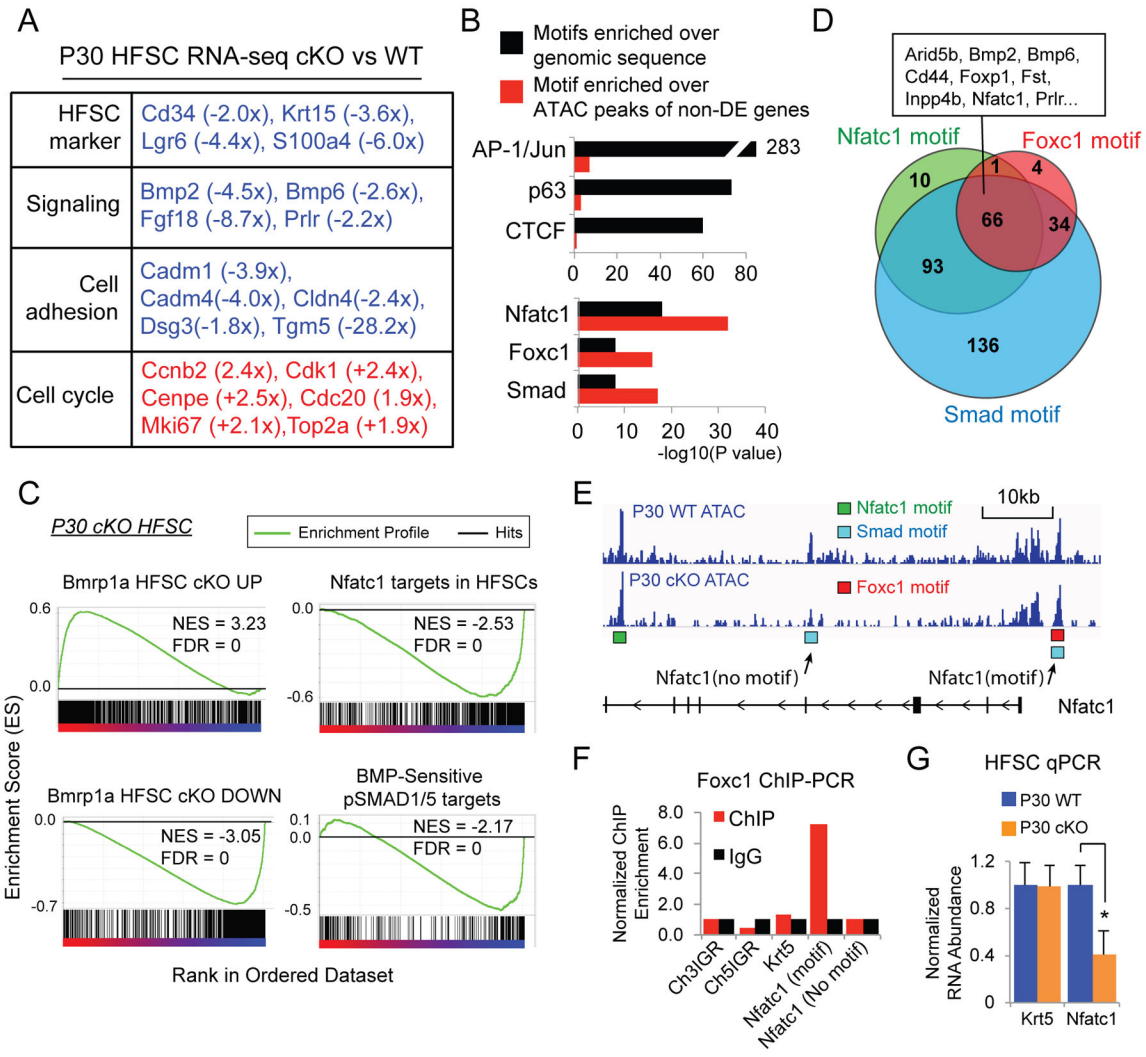

Fig. 4. *Foxc1* activates quiescence gene networks

(A) Functional classification of selected differentially expressed gene in P30 KO HFSCs. **(B)** Comparison of enriched TF motifs against genomic sequences and against the peaks covering the non-differentially expressed (non-DE) genes in P30 KO HFSCs. **(C)** GSEA of BMP responsive genes and Nfatc1 targets in P30 KO HFSCs. **(D)** Venn diagram of the differentially expressed genes in P30 KO HFSCs that contain motifs of Foxc1, Smad and Nfatc1 shows a co-regulated gene network. **(E)** ATAC-seq track of the *Nfatc1* locus. Location of Nfatc1, Smad and Foxc1 motifs are shown in the peak region. **(F)** ChIP-PCR analysis of Foxc1 confirms association of Foxc1 to the predicted binding site in the *Nfatc1* locus. **(G)** Differential expression of Foxc1 targets, *Nfatc1*, in the WT and KO HFSCs (* $p<0.05$).